Biochimica et Biophysica Acta 1797 (2010) 1849–1857

Contents lists available at ScienceDirect

Biochimica et Biophysica Acta

journal homepage: www.elsevier.com/locate/bbabio

How does antimycin inhibit the bc_1 complex? A part-time twin

Stéphane Ransac, Jean-Pierre Mazat *

Université de Bordeaux 2, 146 rue Léo-Saignat, F 33076, Bordeaux cedex, France
Mitochondrial physiopathology laboratory, INSERM U688, Bordeaux, France

ARTICLE INFO

Article history:
Received 19 January 2010
Received in revised form 26 May 2010
Accepted 28 May 2010
Available online 4 June 2010

Keywords:
Gillespie algorithm
bc_1 complex
Antimycin A
Stochastic modelling

ABSTRACT

Using a stochastic simulation without any other hypotheses, we recently demonstrated the natural emergence of the modified Mitchell Q-cycle in the functioning of the bc_1 complex, with few short-circuits and a very low residence time of the reactive semiquinone species in the Q_o site. However, this simple model fails to explain both the inhibition by antimycin of the bc_1 complex and the accompanying increase in ROS production. To obtain inhibition, we show that it is necessary to block the return of the electron from the reduced haem b_L to Q_o. With this added hypothesis we obtain a sigmoid inhibition curve due to the fact that when only one antimycin is bound per bc_1 dimer, the electron of the inhibited monomer systematically crosses the dimer interface from b_L to b_L to reduce a quinone or a semiquinone species in the other (free) Q_i site. Because this step is not limiting, the activity is unchanged (compared to the activity of the free dimer). Interestingly, this b_L–b_L pathway is almost exclusively taken in this half-bound antimycin dimer. In the free dimer, the natural faster pathway is b_L–b_H on the same monomer. The addition of the assumption of half-of-the-sites reactivity to the previous hypothesis leads to a transient activation in the antimycin titration curve preceding a quasi-complete inhibition at antimycin saturation.

1. Introduction

We recently demonstrated [1] that we can explain the bifurcation of electrons in the Q_o site of the bc_1 complex by using a stochastic simulation with the crystal structure, together with the knowledge of the midpoint potentials of the individual redox centres and the ISP head movement. We then observe the natural emergence of the "modified" Mitchell Q-cycle [2–5] with few short-circuits and a low residence time of the reactive semiquinone species in the Q_o site without any other hypotheses. In this model, the two electrons are transferred sequentially from the QH_2 molecule bound in Q_o, but the second electron transfer to b_L follows the first one onto FeS so rapidly that it appears concerted. It is a sequential concerted-like transfer of the two QH_2 electrons. Importantly, the bifurcation of the two QH_2 electrons occurs naturally in Q_o without any gating mechanism to prevent the second electron from following the first one on the FeS-c_1-c pathway (short-circuits [6,7] also called bypasses [8,9]).

However, inhibition of the bc_1 complex by antimycin A cannot be reproduced in this simple model. Furthermore, in our current model, there is not only no inhibition of the bc_1 complex activity by antimycin but also an increase in the activity due to a bypass for the second electron blocked by antimycin on haem b_L.

Indeed, in the framework of Q cycle hypothesis, there is no fundamental reason for which antimycin should inhibit bc_1 complex activity. Antimycin binds to the Q_i site and in principle does not interfere with the bifurcation of the electrons in the Q_o site: while antimycin inhibits one pathway, it does not necessarily inhibit the other one. The electron blocked on b_L by antimycin can return on a semiquinone SQ in Q_o and then follow the high potential pathway (bypass of type 2 or short-circuit 2) [6–9].

Because the inhibition has to be effective in (or close to) the Q_o site and because antimycin binds to the Q_i site far from the Q_o site, many authors have consequently assumed that antimycin binding at Q_i transmits some signal to the Q_o site. Several implicit or explicit hypotheses have been made concerning the nature of this signal. It seems clear that it is not of a transconformational type. To date, no change has been apparent in the different crystal structures where antimycin is bound. However it should be emphasized that the Q_o site in all these structures is also occupied by an inhibitor (stigmatellin) that can block a possible conformational change.

Several authors [6,7,10–13] have underlined the need for gating processes (in Q_o) to avoid bypasses. An attractive hypothesis was put forward by Crofts et al. (reviewed in Ref. [13]). They propose the existence of two subsites in Q_o, one close to FeS (and far from b_L) and the other one close to b_L (and far from FeS). They also assume coulombic interaction between a reduced b_L and the semiquinone SQ in Q_o which should maintain this semiquinone far from the reduced b_L and prevent the electron return from b_L to SQ in Q_o. We study this hypothesis in our model.

* Corresponding author. Inserm U688 Université de Bordeaux 2, 146 rue Léo-Saignat, F 33076, Bordeaux cedex, France. Tel.: +33 557 571 506.
E-mail address: jpm@u-bordeaux2.fr (J.-P. Mazat).

0005-2728/$ – see front matter © 2010 Elsevier B.V. All rights reserved.
doi:10.1016/j.bbabio.2010.05.014

In addition, it has long been known that antimycin inhibition is not necessarily linear in spite of its rather high affinity, but that it could be parabolic (sigmoid). A first explanation was given by Kröger and Klingenberg [14,15] in terms of diffusible quinones: partial inhibition of the bc_1 complex would have no effect on the total electron transfer rate as long as the reaction of the bc_1 complex is not rate-limiting. One would now refer to it as not controlling in the light of metabolic control analysis [16–18]. However, this behaviour is also encountered with the isolated complex, a phenomenon that cannot be explained by the buffering effect of a "quinone pool." This was analyzed by Bechmann et al. [19] who obtained parabolic or linear antimycin inhibition curves, depending upon the different quinols used. With mitochondria from beef heart, the shape of the inhibition curve with antimycin A is parabolic if the quinol-cytochrome *c* reductase turns over at about 300 s^{-1}, but it is hyperbolic if the rate is 5-fold lower. They proposed the new hypothesis of a rapid intra- and inter-dimeric redistribution of antimycin at substoichiometric concentrations exchanging via the lipid phase and substantiated it with a model that accounts well for their results.

Another explanation was developed when the first crystal structures of bc_1 complex became available, showing that the two haem b_L in the dimer were close enough to allow the passage of electrons between each other. Experimental attempts to evidence such passages proved unfruitful, however [11], or were observed only in special conditions [20]. In our simulations reported in Ref. [1], we noted some rare net movement of electrons between the two b_L of the same dimer in accordance with the experimental data. As noted in Ref. [21], the direct electron transfer from haem b_L to haem b_H of the same monomer is promoted, at least in the absence of a proton motive force.

However, as stressed in Ref. [6], the existence of a b_L–b_L transition "helps to explain how the first substoichiometric fraction of antimycin that binds, inhibits noticeably less effectively than the final fraction". These authors also noted that "this removes the strict coupling between two turnovers of one Q_o site and one Q_i site described in the traditional double Q-cycle model". This was also noticed by Covian et al. [22] in support of a more complicated mechanism of half-of-the-sites reactivity for ubiquinol oxidation and rapid electron transfer between bc_1 monomers. They also observed a stimulation of the activity of the bc_1 complex at a substoichiometric fraction of antimycin and proposed that this was a consequence of the half-of-the-sites reactivity. They recently provided new evidence for such mechanism with the elegant construction of a heterodimer [23] in which the stimulation by low antimycin concentrations vanished.

Explaining antimycin inhibition therefore seems crucial in understanding the mechanism of bc_1 complex functioning, because it probably mimics what occurs in the presence of proton motive force when haems b_L and b_H are more reduced than in its absence.

In this paper we use our stochastic model to test some of the hypotheses put forward to explain antimycin inhibition and its peculiar characteristics. We show that preventing the return of the electron from haem b_L to SQ in Q_o is absolutely necessary and also sufficient to obtain antimycin inhibition. The latter is parabolic (sigmoid) due to an increase in b_L–b_L transition when only one antimycin molecule per dimer is bound. We also analyze the effects of the half-of-the-sites reactivity hypothesis on the shape of the antimycin inhibition curve.

2. Methods/model

2.1. Methods/model

The model is fully described in Ref. [1], with some minor changes in the parameters and the rate constants quoted in Tables S1 and S2 in supplementary materials. There was a sign error in Eq. (2) [1] which is corrected below. Simulations made at different substrate concentrations allowed us to evaluate the K_M for substrates. These values depend upon the binding and release rate constants (italicized values in Table S2). They were chosen in order to obtain K_M values similar to those reported in the literature. With the parameter data set listed in Table S2, we obtained $k_{cat} = 182\ s^{-1}$ (per monomer), $K_{M\ QH2} = 3.1\ \mu M$; $K_{M\ cyt\ c} = 2.2\ \mu M$. We also obtained inhibition at a high Q concentration ($K_I = 70\ \mu M$) and a Q activation at low concentration ($K_A = 66\ nM$). The electron tunnelling rate constants from which we derive the probabilities of reactions are calculated according to Moser et al. [24–26]:

$$\log k_{et}^{exer} = 13-(1.2-0.8\rho)(D-3.6)-\gamma\frac{(\Delta G^{o}_{exer}+\lambda)^2}{\lambda} \quad (1)$$

for the exergonic direction of the reactions or:

$$\log k_{et}^{ender} = 13-(1.2-0.8\rho)(D-3.6)-\gamma\frac{(\Delta G^{o}_{exer}+\lambda)^2}{\lambda} + \frac{\Delta G^{o}_{exer}}{0.06} = \log k_{et}^{exer} + \frac{\Delta G^{o}_{exer}}{0.06} \quad (2)$$

for the endergonic direction of the reaction.

"exer" means exergonic and "ender" means endergonic. The $\Delta G°$ values used as well as the distance (D) are shown in Table S2 of supplementary materials.

$\Delta G°_{exer}$ are calculated from the midpoint redox potentials listed in Table S1. ρ is the packing density which is around 0.76 in a typical protein [25]. λ is the reorganization energy (in eV); 0.7 eV seems to be an adequate generic value [25], $\gamma = 4.23\ eV^{-1}$ is derived from the classical Marcus expression [27–29]. Moser et al. [24–26] use $\gamma = 3.1\ eV^{-1}$. When the classical Marcus treatment was used with $\gamma = 4.23\ eV^{-1}$, these two forms of the rate equation (Eqs. (1) and (2)) gave identical results (see the discussion in Ref. [28]). The rate constants (forwards and backwards) in Table S2 used in all our simulations were calculated using Eq. (1) with this latter value of $\gamma = 4.23\ eV^{-1}$.

We used 51 different crystallographic bc_1 structures to calculate the various distances between the redox centres and/or substrates or the products bound in the binding sites. All the 51 structures were used to estimate the b_L–b_L and b_L–b_H distances without weighting the values according to the resolution of the crystallographic structure, because these distances are very reproducible in all structures from all species (12.2 ± 0.2 Å and 13.9 ± 0.4 Å). When the substrates/products are concerned, or the position of the FeS cluster, only part of the set of structure can be used, and sometimes only one.

The time course of the reaction is calculated using the Gillespie algorithm [30] as described in Ref.[1].

We work with only one bc_1 molecule and 300 QH_2 molecules, 100 Q molecules and 600 oxidized cytochrome *c* in a volume $v = 3.3\ 10^{-17}$ L. These values aim at reproducing the in vitro conditions of the enzyme assay (after [31]). Each simulation lasts 0.5 s of reaction time.

To simulate the antimycin inhibition curves, we calculate the concentrations of the different antimycin-bound species of the bc_1 complex E1E2, E1IE2, E1E2I and E1IE2I (I stands for antimycin inhibitor) as in Ref. [31], assuming a total concentration of 50 nM bc_1 complex (Fig. 1; see also an example of such calculations of concentrations in Table S3 in supplementary materials). Then we calculate the mean of 5 time courses for one molecule of each species (one free bc_1, one bc_1 dimer with one antimycin and one bc_1 dimer with two antimycin molecules) and express the resulting activity as the linear combination of the individual average activities proportionally to their concentrations.

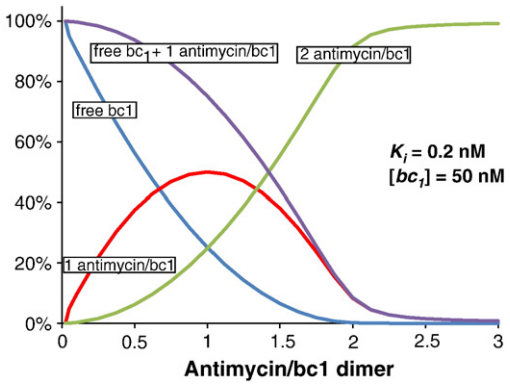

Fig. 1. Distribution of the different antimycin bound bc_1 dimers. The concentrations are calculated as described in Model section with K_i (antimycin) = 0.2 nM and [bc_1] = 50 nM. Free bc_1 in blue, bc_1 dimer with one antimycin molecule in red, bc_1 dimer with 2 antimycin molecules in green, free $bc_1 + bc_1$ dimer with one antimycin molecule in violet.

3. Results and discussion

3.1. The simple model does not account for antimycin inhibition

In the simple stochastic model of bc_1 complex functioning that we proposed in Ref. [1], the primary event is the passage of the first QH_2 electron on FeS. Although the electron transfer is uphill, it is the only possibility (Fig. 2), so it may be one of the controlling steps in the process. Once the first electron has jumped to FeS, three reactions may occur. (i) The most probable is the return of this first electron on SQ to give back QH_2. It is a very likely possibility which occurs many times in our simulation and which brings the system back to its initial state. We will not consider further this situation except for taking into account the delay it introduces in the overall reaction. The other two sequences of events are (ii) the movement of the ISP head towards the cytochrome c_1 taking the electron away from the Q_o site and placing the second electron in the instable SQ in a very favourable position to be transferred to b_L (Figs. 2 and 3A). On the other hand, (iii) the second electron may jump to b_L during the time the first electron is on FeS_Q (close to Q_o) before the head has moved to c_1 (Fig. 3B). In the latter mechanism, as soon as the second electron jumps to b_L, the first one is trapped on FeS because the midpoint potential of Q/SQ becomes quasi unattainable. In both cases, the transfer of the two QH_2 electrons is sequential but so rapid that it may appear as concerted. The choice between these two sequences (Fig. 3A and B) will depend upon the rate of ISP movement. At high rate the first sequence (Fig. 3A) will be triggered while at lower ISP head shift, the other scenario (Fig. 3B) will occur. One or the other of these sequences underpins the mechanism of the Mitchell Q-cycle, which is based on the bifurcation of the electrons at Q_o. This interplay between the rate constants responsible for this concerted-like sequential mechanism has already been described by Rich in Ref. [32] (see beginning of Section 3). In some cases the bifurcation fails in what is called bypasses [8,9] or short-circuits [7]. The most frequent of these are represented in Fig. 4. In type 1 bypass, the second QH_2 electron goes directly to FeS. In type 2 bypass, the second electron returns from the reduced b_L on a new SQ molecule and gives back a new quinol QH_2, one electron of which normally goes to FeS. It is as if the second electron transiently stored on b_L returns to FeS. The number and the type of short-circuits will also somewhat depend upon the ISP head displacement rate. Fig. 5 shows that the global rate of the reaction increases when the displacement velocity of the ISP head increases. This increase is accompanied by a slight increase in both types of short circuits, as shown in Fig. 4. The value of 60,000 s^{-1} given by Millett & Durham for the rate of ISP head movement [33] and represented by a yellow point in Fig. 5 corresponds to the sequence of events B in Fig. 3 (the first electron is trapped on FeS while the second is transferred to b_L). It stands in a region for which the number of short-circuits is low. In the following we take this value of 60,000 s^{-1} for the ISP head displacement (in both directions).

However, in the presence of antimycin, the simulations conducted with this model do not evidence any inhibition (Fig. 6). On the contrary, the rate increases due to an increase in type 2 bypass (blue curve on Fig. 6), because in the presence of antimycin, the haem b_L is mainly reduced. At antimycin saturation, all the QH_2 electrons go to FeS and then to c_1 and c, one directly and the other one through b_L (type 2 bypass). The number of bypasses is exactly half of the number of reduced cytochrome c (Fig. 6). We then observe an increase in the rate because both electrons of each QH_2 reduce two cytochrome c molecules instead of one in the normal functioning of the complex.

3.2. What are the characteristics of antimycin inhibition?

To explain the role of antimycin, we have to take into account the following salient features of antimycin inhibition: (i) its inhibitory effect i.e. a decrease (close to zero) in the activity of the bc_1 complex; (ii) the ROS production associated with antimycin binding and presumably following an increase in semiquinone SQ at Q_o; and (iii) the oxidant-induced reduction of bc_1 complex [34,35], i.e. the fact

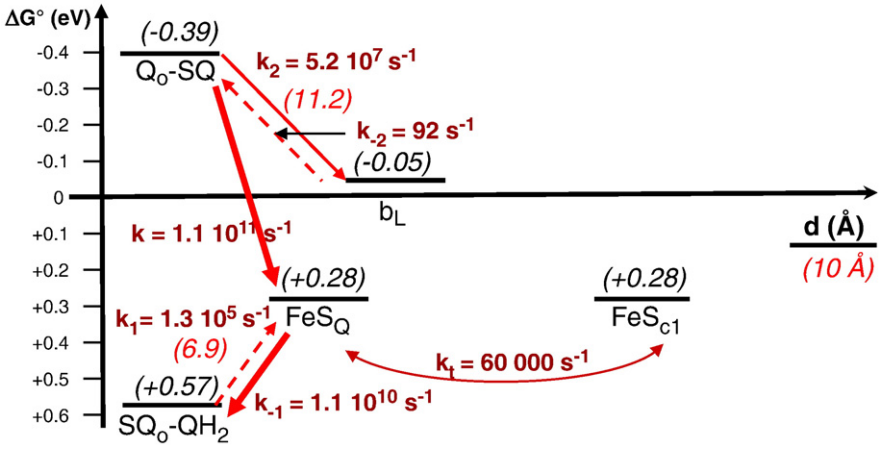

Fig. 2. The energetics of the electron transfers at the Q_o site. The values in brackets in black italics above the sites are the midpoint potentials of the redox couples. The values in red italics and in brackets along the arrows are the distances between the redox centres. The rate constants are indicated in dark red along the arrows. The thickness of the arrows is related to the intensity of the rate constants. Dotted arrows correspond to unfavoured events.

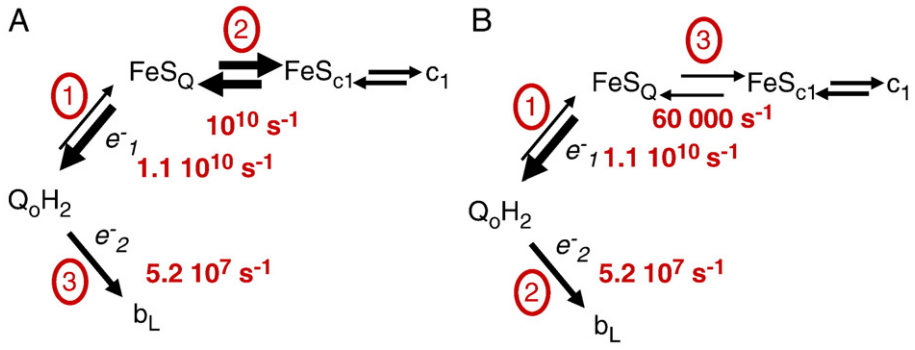

Fig. 3. Sequences of electron transfers at Q_o depending on the rate of ISP head displacement. The thickness of the arrows is proportional to the probability of transfer. (A) Rapid motion of the ISP head. (B) Slow motion of the ISP head (60,000 s^{-1} as reported in Ref. [33]).

that, in the presence of antimycin, oxygen and a respiratory substrate, b-type haems are reduced whereas cytochrome c_1/*c* are oxidized.

As detailed in Introduction, several models have been proposed to account implicitly or explicitly for antimycin inhibition. They form two main types: (i) models which assign to b_L, when reduced, special effects on the electron (and proton) movements in Q_o [10–13,27,36–38]; (ii) models which involve a kind of half-of-the-sites reactivity, implying that only one monomer of the bc_1 dimer is active at a time [20,22,23,31,39].

We describe in more detail the features of the first class of models and analyse their consequences with the help of our stochastic model. In this way, we can explore the mechanism of electron transfers at Q_o site. Finally we study the consequences of introducing half-of-the-sites reactivity on antimycin inhibition.

3.3. Two subsites in Q_o?

Based on the structures of the Q_o site and on the observation that there are two classes of inhibitors with different binding in the Q_o site producing different effects, Crofts and others proposed that there are two subsites in Q_o, one close to the FeS (7 Å from FeS and 12.4 Å from b_L) called the distal site (from b_L; we refer to it as Q_{of}) and the other close to b_L called the proximal site (we refer to it as Q_{ob}) (6.3 Å from b_L) [10–13,27,40,41]. The idea is that QH_2 binds first to Q_{of} close to FeS, gives its first electron to FeS, becoming SQ, which moves to Q_{ob} close to b_L thereby giving it its second electron. In other words, the quinol/semiquinone molecule is always close to the acceptor to which it gives its electron. Hong et al. [41] "favoured this mechanism because of the need to minimize harmful short-circuit reactions by keeping [SQ] occupancy to a minimum" [13]. To test this hypothesis, we added into our simple model the presence of two subsites Q_{of} and Q_{ob} with a possible stochastic transfer of the quinone Q/semiquinone SQ from one site to the other (QH_2 is thought to remain in Q_{of}). Fig. 7 represents the activity of the reaction as a function of the distance between the two sub sites (i.e. the distance Q_{of}–Q_{ob}). We start at the Q_o position of our model (Q/SQ/QH_2 at 6.9 Å from FeS and 11.2 Å from b_L) [1], i.e. assuming that the two sites overlap, then we move Q_{ob} away from Q_{of} (Q_{of} remains at its initial position) and we study the rate of the global reaction, the possible short-circuits and the residence time of SQ at Q_o.

As shown in Fig. 7, the behaviour depends upon the rate of quinone species displacement between the two subsites. When the rate is slow, the second electron although far from b_L (11.2 Å) is able to jump to b_L from position Q_{of} before the SQ molecule moves to Q_{ob}. In this case, the rate of the global reaction activity is unchanged. When the rate of quinone species displacement between both sites is increased, the transfer of the second electron is facilitated (closer to b_L) so the activity is increased (with no significant changes in the residence time of the semiquinone at Q_o (not shown)). This could explain the higher activity observed in the Rhodobacter bc_1 complex in pre-steady state experiments [29]. An enhancement of the rate constant of b_L reduction due to a movement of SQ inside Q_o was already proposed by Crofts et al. a long time ago (see the discussion in Ref. [11,13,41,42]). However, even if we suppose that, for reasons of charge repulsion, SQ is confined to Q_{of} far from reduced b_L, adding antimycin does not prevent the electron of reduced b_L from jumping to SQ to begin the short-circuit of type 2, leading to an increase in activity, as in the simple model (compare Figs. 8 and 6).

Thus even an SQ distance of approximately 12 Å from the reduced haem b_L does not in itself impede the back flow of the b_L electron on SQ and does not lead to antimycin inhibition. Another hypothesis is therefore required.

3.4. A hypothesis for obtaining antimycin inhibition

Although the two Q_o subsites hypothesis is not a satisfactory explanation for antimycin inhibition, it does again show that one

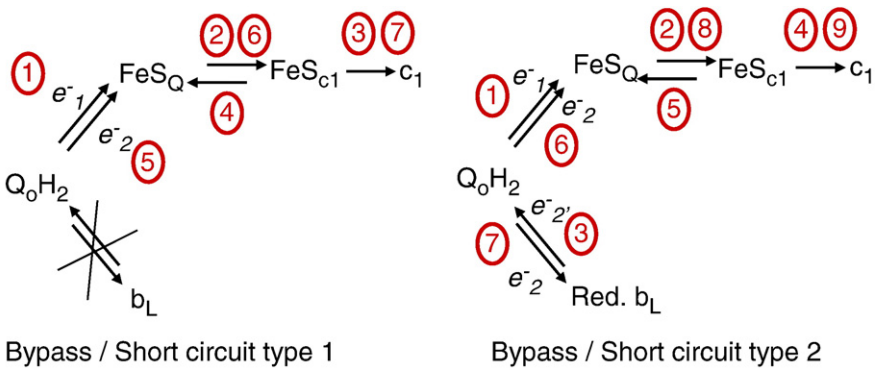

Fig. 4. Short-circuits (bypasses) that can occur at Q_o (type 1 and type 2). The order of electron transfer is indicated by the circled red digits. In type 2 short-circuit, a prime is added to electron 2, $e_{-2'}$, because it is normally the second electron of a previous QH_2 molecule.

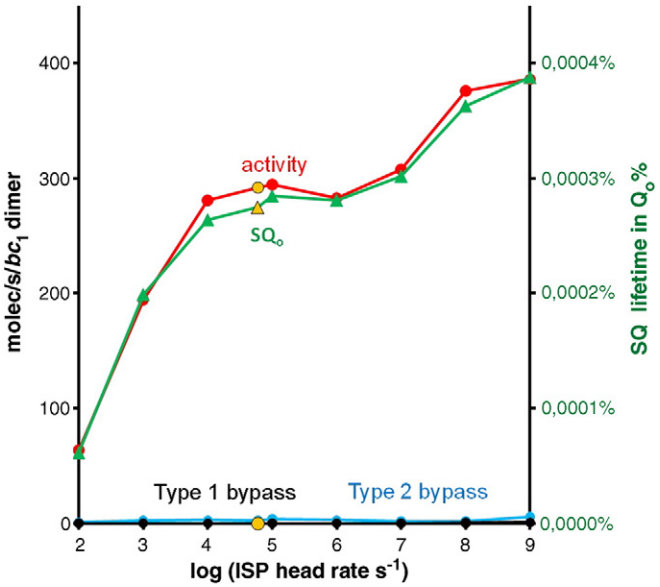

Fig. 5. Effect of the speed of ISP head displacement on the global rate constant. Red (circle), left scale bc_1 activity (cytochrome c reduced per second); green (triangle), right scale, SQ lifetime in Q_o; black, left scale number of type 1 bypasses per second (SQ ➔ FeS); blue type 2 bypasses (b_L ➔ SQ). The large yellow point corresponds to the 60,000 s^{-1} value taken in the following according to [33].

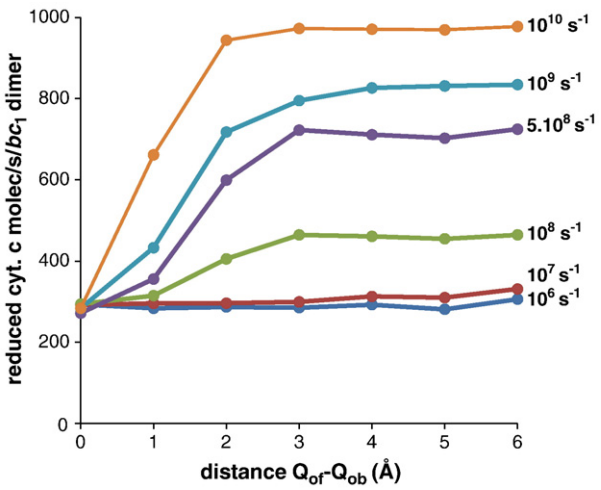

Fig. 7. Effect of the distance between two subsites at Q_o. In abscissa the distance between two subsites Q_{of} close to FeS and Q_{ob} close to haem b_L. The origin corresponds to the two sites overlapping the initial position as in Fig. 6 (6.9 Å from FeS and 11.2 Å from b_L). The Q_{of} site is conserved in this position and the Q_{ob} site is displaced from the distance indicated in abscissa in the direction to b_L, so that the distance $(Q_{of}-Q_{ob})+(Q_{ob}-b_L)=11.2$ Å. The different curves correspond to different rates of transition of the SQ molecules (and possibly of all other species of quinone/quinol) between both sites.

reason for the absence of inhibition and the increase in the global activity of bc_1 complex is the existence of type 2 bypass when b_L is maintained reduced (Figs. 6 and 8). Thus we must suppose that for some reason, when b_L is reduced, the b_L electron cannot return to the SQ at Q_o. This hypothesis was already suggested by Crofts et al. [13].

Fig. 9 shows that this hypothesis is sufficient to obtain antimycin inhibition provided that both antimycin sites are occupied. The reason for the inhibition is that the Q_o site is mainly occupied by QH_2 (Table 1) because the electron jump to FeS is not facilitated owing to its higher midpoint potential. The first QH_2 electron can no longer be trapped at FeS by the passage of the second electron on the haem b_L, which is already reduced in the presence of antimycin. The situation is thus: (FeS_{ox}–QH_2–b_{Lred}) with some short and rapid transitions to (FeS_{red}–SQ–b_{Lred}), which quickly return to the previous situation faster than the head motion. Thus FeS is mainly oxidized (see Table 1) and its displacement to c_1, if any, has little chance of carrying any electron. For this reason, the reduction of b_L in the absence of antimycin, and presumably the reduction of b_H which follows very rapidly, normally precede the reduction of c_1, as observed by Yu et al. [36,37]. This is because the electrons move faster than the ISP head and do not necessarily cause ISP head motion. However, in the presence of only one antimycin per dimer, we found paradoxically that the catalytic rate is not affected ($288.4\pm12.8\ s^{-1}$ for the free dimer and $288.0\pm9.4\ s^{-1}$ for the dimer with only one bound

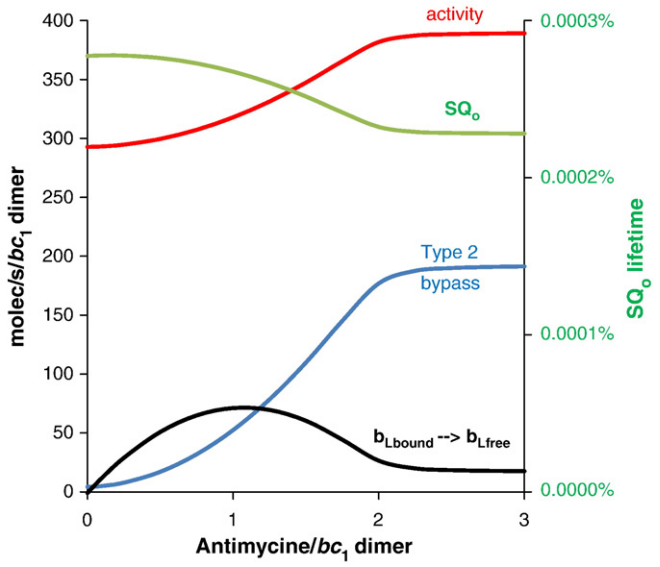

Fig. 6. Effect of antimycin with the simple model described in [1]. Left scale: In red: activity in s^{-1}; in blue, number of type 2 bypasses per second (b_L ➔ SQ); the black bell-shape curve, b_{Lbound} ➔ b_{Lfree}, indicates the net number of b_{L2} ➔ b_{L1} transitions per second (antimycin in Q_{i2}) + net number b_{L1} => b_{L2} transitions per second (antimycin in Q_{i1}). Right scale (in green): lifetime of semiquinone at Q_o.

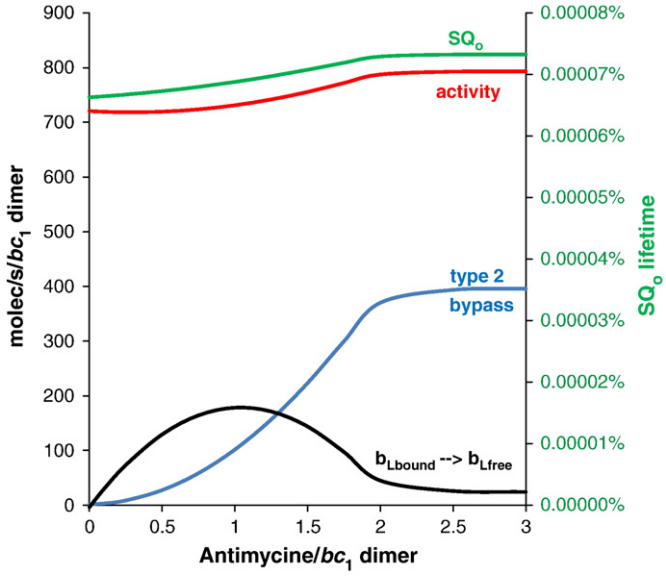

Fig. 8. Effect of antimycin on the two Q_o subsites model. The quinone species displacement rate between the two subsites Q_{of} and Q_{ob} (distant from 5 Å) is $5.10^8\ s^{-1}$. Colour as in Fig. 6. In red, left scale, activity in s^{-1}; in blue, left scale, number of type 2 bypasses per second (b_L ➔ SQ); in black, left scale, net number of b_{Lbound} ➔ b_{Lfree} transitions per second; in green, right scale, lifetime of semiquinone at Q_o (SQ on right scale).

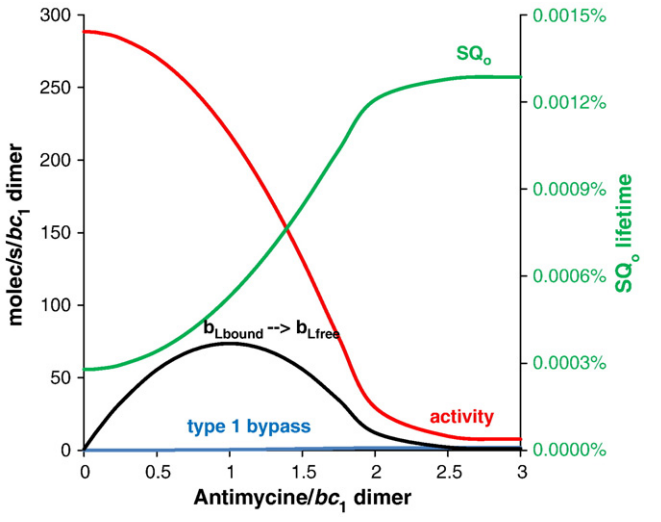

Fig. 9. Proposed model of antimycin inhibition. In this model it is assumed that the return of the second electron of b_{Lred} on $SQ^{\bullet -}$ is impossible. The colours are the same as in Fig. 6: activity (red curve, left scale); time residence of SQ in Q_o (green curve, right scale). The black curve (left scale) indicates the net number of $b_{Lbound} \rightarrow b_{Lfree}$ transitions per second. The blue curve indicates the low number of SQ ➔ FeS bypass due to a low probability of return of the b_L electron on a Q molecule at Q_o through a transient formation of a semiquinone molecule SQ (See Fig. 11) in Q_o which immediately gives its electron to FeS.

antimycin; the activity of the dimer with 2 antimycins is 5 s^{-1}), so the inhibition curve of Fig. 9 is more or less similar to the "free $bc_1 + 1$ antimycin/ bc_1" curve in Fig. 1 in line with experimental results (e.g. [19]).

When looking for the sequence of electrons transfers in the half-occupied dimer, we found an abnormally high number of i) $b_{L2} => b_{L1}$ net passages when antimycin was bound to monomer 2 and ii) net passages $b_{L1} => b_{L2}$ when antimycin was bound to monomer 1 (amounting to 147 ± 12 per second for the full activity of 288 ± 9 s^{-1}). This means that the Q_o site of the monomer occupied by antimycin functions normally like the Q_o site of the other (free) monomer, but with its second electron going to the Q_i site of the other monomer (see Fig. 10). This is in line with the observation that a controlling step of the process is the transfer of the first electron to FeS. Even if the $b_{L1} <=> b_{L2}$ transition is not rapid, it is faster than the steps involved in the high potential pathway ($Q_o => FeS => c_1 => c$), so two such events have time to occur meanwhile at Q_{i1} (resp. Q_{i2}). In the free dimer, the cross route $b_{L1} <=> b_{L2}$ is more rarely used because the $b_L => b_H$ route is faster. However, if this $b_L => b_H$ electron transfer is slowed down in the free dimer, e.g. due to the setting up of the membrane potential, the $b_{L1} <=> b_{L2}$ transition could be favoured again, but in this case with an equal passage in both directions (see the discussion in Ref. [21]).

This behaviour gives the antimycin inhibition curve its cooperative shape (Fig. 9) and fulfils the two other salient features of antimycin inhibition: the increase in the lifetime of SQ at the Q_o site (green curve on Fig. 9) and the oxidant-induced reduction of cyt b (Table 1).

In our conditions, inhibition is not complete. This is partly due to the 0.8% half-inhibited enzyme still present at an antimycin/bc_1 ratio of 3 (see Table S3 of supplementary data) but also to a rare bypass represented in Fig. 11 in which there occurs the release of QH_2 from Q_o and its replacement by a quinone Q. Although it is very unfavourable the Q molecule can now accept the electron from the reduced b_L to form SQ and give it immediately to FeS to give back Q. Because b_L is now oxidized, a normal cycle of reactions can then occur with another reduction of cytochrome *c*. The residual activity is thus twice the number of bypasses. This possibility is favoured in our

Table 1
Occupation of the different sites Q_O and Qi and redox states of the redox centres in the two monomers 1 and 2. E1E2 depicts the free bc_1 dimer. E1E2I (equivalent to E1IE2) depicts the bc_1 dimer with one antimycin. E1IE2I depicts the bc_1 dimer with two antimycins. Two models are envisaged. In the first model the return of the b_L electron is forbidden as in Fig. 8. In the second model, a half-of the-sites mechanism is also hypothesized in addition to the non-return of the b_L electron (Fig. 9).

			Q_o site			Q_i site											Cyt. c site		
			Free	QH_2	SQ	Q	Free	QH_2	SQ	Q	Antimycin	Red. b_L	Red. b_H	Oxi. prox. FeS	Red. prox. FeS	Oxi. dis. FeS	Red. dis. FeS	Red. C_1	Free	Oxi. Cyt c	Red. Cyt c
Bypass type II forbidden	Monomer 1	E1E2	21.9%	71.5%	0.00028%	6.6%	8.5%	0.8%	17.7%	72.9%	0%	0.31%	34.3%	25.6%	24.4%	25.6%	24.4%	13.8%	10.2%	74.8%	15.0%
		E1E2I	21.3%	73.0%	0.00026%	5.7%	10.6%	1.6%	17.3%	70.4%	0%	0.48%	33.7%	23.8%	26.1%	24.2%	26.0%	14.0%	10.3%	74.6%	15.2%
		E1IE2I	11.9%	86.7%	0.00115%	1.4%	0%	0%	0%	0%	100%	99.4%	100.0%	49.5%	0.53%	49.5%	0.53%	0.24%	6.6%	93.1%	0.27%
	Monomer 2	E1E2	22.6%	71.4%	0.00028%	6.0%	8.6%	0.8%	16.3%	74.2%	0%	0.30%	31.6%	25.4%	24.3%	25.9%	24.4%	12.9%	11.1%	74.9%	14.0%
		E1E2I	22.9%	70.9%	0.00029%	6.2%	0%	0%	0%	0%	100%	2.0%	78.2%	26.1%	24.1%	26.2%	23.6%	13.0%	10.1%	75.9%	14.0%
		E1IE2I	12.5%	86.1%	0.00143%	1.5%	0%	0%	0%	0%	100%	99.4%	100.0%	49.5%	0.57%	49.4%	0.57%	0.26%	6.7%	93.0%	0.29%
Bypass type II forbidden + half-of-the-site reactivity	Monomer 1	E1E2	78%	20.2%	0.00011%	1.7%	24.0%	0.4%	12.4%	63.2%	0%	1.1%	32.7%	40.6%	9.4%	40.9%	9.1%	4.3%	7.3%	88.0%	4.7%
		E1E2I	21%	74.0%	0.00030%	5.2%	35.2%	1.0%	13.1%	50.6%	0%	7.0%	44.6%	26.4%	23.6%	26.6%	23.4%	12.7%	11.1%	75.2%	13.7%
		E1IE2I	12%	86.3%	0.00148%	1.5%	0%	0%	0%	0%	100%	99.3%	100.0%	49.4%	0.59%	49.5%	0.59%	0.27%	6.7%	93.0%	0.30%
	Monomer 2	E1E2	82%	16.2%	0.00009%	1.7%	28.0%	0.3%	12.0%	59.8%	0%	1.2%	34.2%	41.4%	8.4%	41.9%	8.3%	4.2%	8.4%	87.0%	4.6%
		E1E2I	72%	26.3%	0.00014%	1.9%	0%	0%	0%	0%	100%	7.4%	67.4%	38.6%	11.5%	38.5%	11.4%	5.2%	7.9%	86.4%	5.7%
		E1IE2I	12%	86.0%	0.00134%	1.5%	0%	0%	0%	0%	100%	99.3%	100.0%	49.4%	0.59%	49.4%	0.59%	0.27%	6.7%	93.0%	0.31%

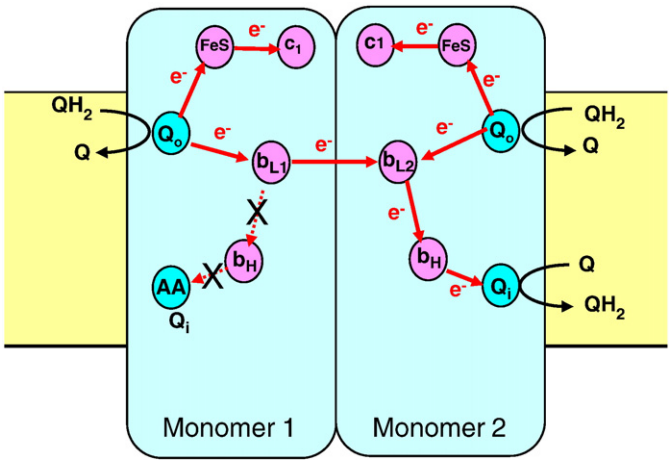

Fig. 10. Scheme of the oriented passage b_{L1} ➔ b_{L2} from the inhibited monomer to the free monomer.

simulations in which the quinone Q concentration is comparable to the quinol QH_2 concentration. In physiological conditions with antimycin, Q will be reduced by complex I or II in QH_2 and the antimycin inhibition will appear nearly complete.

The transition b_{L2} => b_{L1} or b_{L1} => b_{L2} in the half-inhibited dimer is a natural mechanism that can simply account for the sigmoid shape of the antimycin curve.

However, the transition b_L <=> b_L is controversial and seems difficult to evidence experimentally. For instance, in the presence of saturating amounts of antimycin, a linear decrease of the b_H reduction as a function of myxothiazol concentration was observed by Crofts et al. (see Fig. 4 in [11]). This means that no electron from a free Q_o site jumped to the b_L of the other monomer of a myxothiazol-bound site at least during the first 20 ms of measurement.

This leads us to discuss other models which have been proposed, particularly the one by Kröger and Klingenberg [14,15] who explain this non-hyperbolic inhibition in terms of a diffusible ubiquinone and QH_2 connecting the respiratory chain complexes. Bechmann et al. [19] explain this inhibition pattern by assuming that "antimycin A moves rapidly between the inhibition sites at the centre i of the dimeric enzyme". They also hypothesize a fast electron transfer between the two haems b_H of the dimer in the presence of only one bound antimycin.

Both groups noted that the shape depends intriguingly upon the type of quinone used. For example, Bechmann et al. [19] linked the

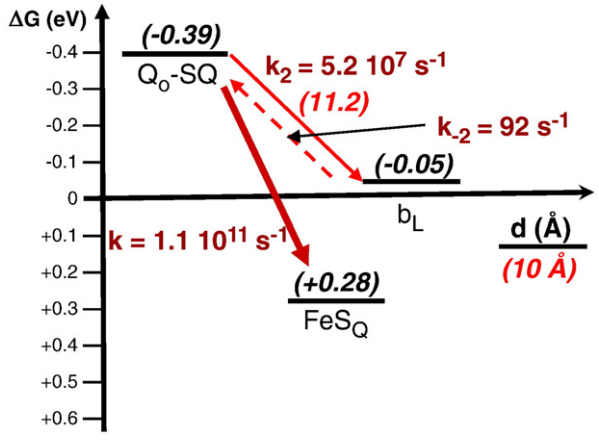

Fig. 11. Bypass of a b_L electron on a Q molecule bound to Q_o (uphill, low probability) followed by its rapid transfer to FeSox (downhill) through the transient formation of a semiquinone. This bypass is slightly favoured in our simulations where we took [Q] is not negligible.

parabolic shape of the curve to a high activity of the bc_1 complex, a hyperbolic curve being recorded with less efficient quinone. This could mean that the affinity of these different quinones or their redox potential [15] might play a role in shaping the antimycin response. Indeed, any factors (affinity or redox potential) reducing their reduction rate in Qi will increase the reduction of b_H and thus b_L on the same monomer and then decrease the possible occurrence of b_L => b_L transfer from the other monomer, thus decreasing the global activity. Fig. 13A simulates the effect of a decrease in quinone affinity to the Q_i site and demonstrates a clear transition from a sigmoid to a hyperbolic shape associated with a decrease in the activity. The situation is somewhat more complex with the additional hypothesis of a half-of-the-sites mechanism as shown in Fig. 13B and discussed below.

3.5. Are there any molecular indications for the non-return of the electron from b_L red?

It can be reasonably assumed that for reasons of coulombic repulsion, $SQ^{\bullet -}$ remains in the Q_{of} subsite as far as possible from a reduced b_L [13,27]. We already demonstrated that the existence of a Q_o subsite far from b_L is not sufficient in itself to impede the return of electrons from haem b_L on a semiquinone species SQ in Q_o.

Another hypothesis is the impossibility for an electron to return without being accompanied by a proton, because the Q^{2-} species (corresponding to the reduction of the $SQ^{\bullet -}$ species) is improbable [32]. Indeed, one of the H^+ coming from QH_2 is supposed to be transferred with its electron to the ISP head (FeS and His 161) and the second H^+ is supposed to take a proton pathway close to haem b_L [13]. This last H^+ which has escaped might not be available to return with the b_L electron to $SQ^{\bullet -}$ (see the discussion of proton release in Ref. [42] and the double-gated model in Ref. [7]). Furthermore, the proton return to SQ could be different in the different positions Q_{of} and Q_{ob} possibly occupied by the semiquinone. Thus, the transition of SQ between the two positions might participate in the gating process and prevent the type 2 short circuit.

3.6. What brings about a half-of-the-sites reactivity in this model?

We showed that the blockage of the electron return from the reduced haem b_L on a semiquinone molecule at Q_o site is necessary to obtain antimycin inhibition. This inhibition curve is sigmoid since the electrons are able to take the cross route b_{L1} <=> b_{L2}. However, we did not observe the transient activation reported by the group of Trumpower [23,31]. To explain this transient activation, they proposed that “whereas free dimers have only one centre P (Q_o) site active at a time, binding of antimycin to one centre N (Q_i) activates the second centre P site, allowing ubiquinol oxidation to proceed in both monomers simultaneously“. We introduced this half-of-the-sites reactivity into our model by assuming that the Q_{o1} and Q_{i2} sites on the one hand, and the Q_{o2} and Q_{i1} sites on the other, cannot be occupied simultaneously. This idea comes from the observation that there are two symmetrical cavities inside the bc_1 complex created by the association of two monomers to form the dimer molecule. One cavity contains the Q_{o1} and Q_{i2} sites; the other, which is symmetrical and independent, contains the Q_{o2} and Q_{i1} sites. Although these cavities seem quite large, the bulky tail of two UQ_{10} molecules might exert steric constraints on them, leading to this alternative binding. However, this does not hold for antimycin which has no cumbersome tail. For instance, antimycin bound at Q_{i2} will not hinder the binding of QH_2 at Q_{o1} (nor of course at Q_{o2}), so the activity could be increased just by doubling the Q_o binding sites in the presence of one molecule of antimycin/bc_1 dimer. Adding this type of half-of-the-sites reactivity to the non-return of b_L electron on a semiquinone in Q_o gives the curve in Fig. 12 (red curve) showing a transient activation followed by a quasi-complete inhibition when all the Q_i sites are saturated with

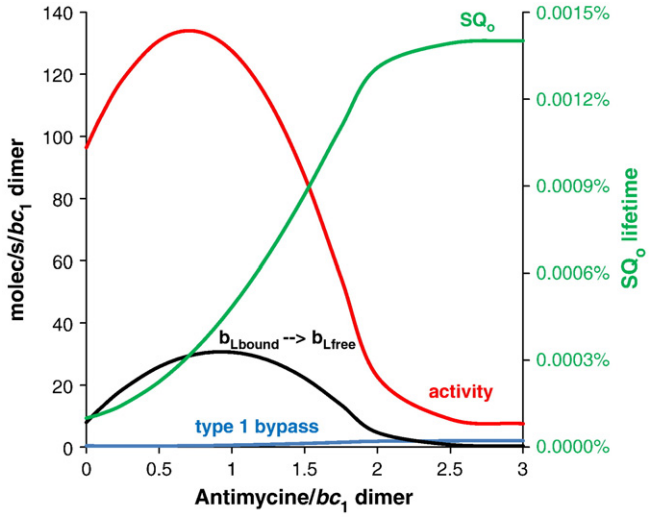

Fig. 12. Proposed model of antimycin inhibition with half-of-the-sites reactivity. This model assumes that the return of the second electron of b_{Lred} on $SQ^{\bullet-}$ is impossible as in Fig. 9. It also assumes that Q_{o1} and Q_{i2} on the one hand and Q_{o2} and Q_{i1} on the other hand cannot be bound simultaneously due to steric hindrance. This does not apply to antimycin which has no bulky tail. Red curve, left scale: activity; green curve, right scale: time residence of SQ in Q_o. The black curve (left scale) indicates the net number of $b_{Lbound} \rightarrow b_{Lfree}$ transitions per second. Blue: bypass $b_L \rightarrow Q \rightarrow FeS$ described in Fig. 11.

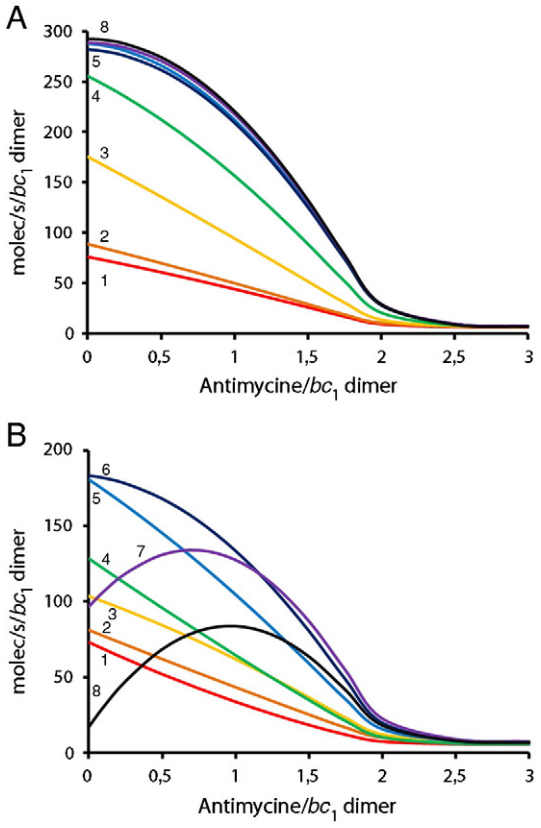

Fig. 13. Inhibition pattern dependency for (A) model presented in figure 9 and (B) model presented in figure 12 (half-of-the-sites reactivity), as a function of the binding of quinone/quinol in Q_i. Binding rate constants have been modified by the following factors: 1/10000 (red, curve 1); 1/1000 (orange, curve 2); 1/100 (yellow, curve 3); 1/40 (green, curve 4); 1/10 (blue, curve 5); 1/4 (indigo, curve 6); 1 (violet, curve 7); 10 (black, curve 8). Rainbow colors (from red to violet) are from the lowest binding rate constant to the highest one.

antimycin. This transient antimycin activation corresponds to only one antimycin molecule bound to the dimer of bc_1, e.g. the Q_{i2} site. In the absence of antimycin, because there is some quinone occupation of the Q_i sites, the Q_o occupation of the other monomer by QH_2 is impeded, as can be seen in Table 1. For instance, 16 to 20% of $Q_{o1}H_2$ or of $Q_{o2}H_2$ (7^{th} line of Table 1) as compared to 71% (1^{st} line of Table 1) where no constraint is introduced. Thus, even in the absence of antimycin, a lower activity in this model (Fig. 12) is observed when compared to the model without binding constraints (Fig. 9). When antimycin is present on only one monomer of the bc_1 dimer, say on Q_{i2}, monomer 1 is now fully active, because the antimycin at Q_{i2} does not impede the binding of QH_2 at Q_{o1} (nor at Q_{o2}, see the discussion above). Monomer 2 (with antimycin) can function more or less normally except that it functions with Q_{i1} (as in the model of Fig. 9). The result is an activation for the bc_1 dimer which contains only one antimycin molecule.

Thus we show that the hypothesis of half-of-the-sites reactivity proposed in Refs. [23,31,39], together with the hypothesis of the non-return of the electron of reduced b_L on a semiquinone at Q_o, accounts quite well for the transient activation of the bc_1 complex activity by antimycin. Obtaining antimycin activation with this model does not irrefutably demonstrate the half-of-the-sites reactivity mechanism, but it is nevertheless a strong indication of its possibility.

However, several authors did not find any activation feature in the antimycin inhibition pattern. Fig. 13 shows that this particular inhibition pattern is highly dependent upon the binding constant of quinone/quinol in Q_i. These simulations demonstrate that the activation feature in the antimycin inhibition pattern (i) is visible only with the half-of-the-sites reactivity hypothesis (Fig. 13B), and that (ii) it depends upon quinone affinity. It can be lost at lower affinity even with the half-of-the-sites reactivity hypothesis. As noted above, the latter observation could explain the different shapes of the experimental curves obtained by Bechman et al. [19] in the presence of different substrates.

4. Conclusion

A simple model can explain the bifurcation of electrons at Q_o due to a subtle distribution of the probabilities of electron transfer between the different redox centres. However, there is no underlying reason why, in this model, antimycin should inhibit bc_1 complex activity. On the contrary, we obtained activation due to the fact that in the presence of antimycin, the second electron bypasses transiently through b_L to FeS and cytochromes c_1 and c, even if the semiquinone is far from the reduced b_L in a distal Q_o subsite. To avoid this bypass, the remoteness of the semiquinone in a Q_o subsite distal from the reduced b_L is not a sufficient explanation. It is necessary that the return of the electron from b_L on the semiquinone SQ cannot occur. We demonstrate here that this hypothesis is sufficient to obtain antimycin inhibition provided that both Q_i sites of the dimer are occupied. It also shows that the passage of the second electron on b_L, which is prevented in the presence of saturating amounts of antimycin, is essential to trap the first electron on FeS and to allow its transfer to c_1. Otherwise, FeS remains oxidized most of the time (Table 1) and unable to transfer an electron to c_1. This is the main reason for antimycin inhibition. With only one antimycin site per dimer, the activity is the same (Fig. 9) or higher if we assume the existence of half-of-the-sites reactivity (Figs. 12 and 13) due to a large increase in net non-limiting $b_{L1} <=> b_{L2}$ transitions in the direction of the free Q_i site.

The model and the hypothesis on which it is based must now be tested by their predictions. The first consequence of this hypothesis is the large increase in $b_{L1} <=> b_{L2}$ transition for those dimers bound with only one antimycin molecule. Such peculiar behaviour in the case of one antimycin per dimer has to be systematically studied in presteady-state kinetics and in the mutants already available. New

mutants could also be designed on the basis of this hypothesis, i.e. mutants impeding the transition b_{L1} <=> b_{L2}. They should transform the allosteric shape of antimycin inhibition into a hyperbolic one. Mutants or drugs could be imagined that facilitate the return of the electron from b_L. Such mutants should grow perfectly in the presence and binding of antimycin without ROS production. The degree of occupancy of Q_o by QH_2 could also be measured. In the half-of-the-sites model it should be dependent on the degree of antimycin saturation. This would not be the case if the monomers were independent, so the QH_2 occupancy at Q_o would be higher (Table 1).

In summary, we underline the interest of our stochastic approach which does not discard a priori any possible reaction and considers what actually occurs in a single bc_1 molecule. In order to obtain antimycin inhibition, our model demonstrates the absolute necessity of a gating mechanism preventing the return of electrons from b_L to a semiquinone in Q_o. The parabolic inhibition of antimycin can be reproduced and depends upon the quinone used (i.e. its affinity for the Q_i site). The introduction of half-of-the-sites reactivity evidences a stimulation of the bc_1 complex activity in the presence of substoichiometric concentrations of antimycin.

Acknowledgments

We are indebted to R. Cooke and D. Fell for revising the English. This work was supported by a grant from ANR/BBSRC SysBio MitoScoP and by the “Ateliers epigenomic”, Genopole and University of Evry.

Appendix A. Supplementary data

Supplementary data associated with this article can be found, in the online version, at doi:10.1016/j.bbabio.2010.05.014.

References

[1] S. Ransac, N. Parisey, J.-P. Mazat, The loneliness of the electrons in the bc_1 complex, Biochim. Biophys. Acta 1777 (2008) 1053–1059.
[2] P. Mitchell, Possible molecular mechanisms of the protonmotive function of cytochrome systems, J. Theor. Biol. 62 (1976) 327–367.
[3] B.L. Trumpower, The Protonmotive Q Cycle, J. Biol. Chem. 265 (1990) 11409–11412.
[4] A.R. Crofts, S.W. Meinhardt, K.R. Jones, M. Snozzi, The role of the quinone pool in the cyclic electron-transfer chain of *Rhodopseudomonas sphaeroides*: a modified Q-cycle mechanism, Biochim. Biophys. Acta 723 (1983) 202–218.
[5] A.R. Crofts, The Q-cycle. A personal perspective, Photosynth. Res. 80 (2003) 223–243.
[6] A. Osyczka, C.C. Moser, F. Daldal, P.L. Dutton, Reversible redox energy coupling in electron transfer chains, Nature 427 (2004) 607–612.
[7] A. Osyczka, C.C. Moser, P.L. Dutton, Fixing the Q cycle, Trends Biochem. Sci. 30 (2005) 176–182.
[8] F. Muller, A.R. Crofts, D.M. Kramer, Multiple Q-cycle bypass reactions at the Q_o-site of the cytochrome bc_1 complex, Biochemistry 41 (2002) 7866–7874.
[9] D.M. Kramer, A.G. Roberts, F. Muller, J. Cape, M.K. Bowman, Q-cycle bypass reactions at the Q_o site of the cytochrome bc_1 (and related) complexes, Methods Enzymol. 382 (2004) 21–45.
[10] A.R. Crofts, The cytochrome bc_1 complex: function in the context of structure, Ann. Rev. Physiol. 66 (2004) 689–733.
[11] A.R. Crofts, J.T. Holland, D. Victoria, D.R.J. Kolling, S.A. Dikanov, R. Gilbreth, S. Lhee, R. Kuras, M.G. Kuras, The Q-cycle reviewed: how well does a monomeric mechanism of the bc_1 complex account for the function of a dimeric complex? Biochim. Biophys. Acta 1777 (2008) 1001–1019.
[12] A.R. Crofts, The bc_1 complex: what is there left to argue about? in: M. Wikström (Ed.), Biophysical and Structural Aspects of Bioenergetics, Royal Society of Chemistry Publishing, Cambridge, 2005, pp. 123–155.
[13] A.R. Crofts, S. Lhee, S.B. Crofts, J. Cheng, S. Rose, Proton pumping in the bc_1 complex: a new gating mechanism that prevents short circuits, Biochim. Biophys. Acta 1757 (2006) 1019–1034.
[14] A. Kröger, M. Klingenberg, The kinetics of the redox reactions of ubiquinone related to the electron-transport activity in the respiratory chain, Eur. J. Biochem. 34 (1973) 358–368.
[15] A. Kröger, M. Klingenberg, Further evidence for the pool function of ubiquinone as derived from the inhibition of the electron transport by antimycin, Eur. J. Biochem. 39 (1973) 313–323.
[16] H. Kacser, J.A. Burns, The control of flux, Symp. Soc. Exp. Biol. 32 (1973) 65–104.
[17] R. Heinrich, T.A. Rapoport, A linear steady-state treatment of enzymatic chains. General properties, control and effector strength, Eur. J. Biochem. 42 (1974) 89–95.
[18] C. Reder, Metabolic control theory: a structural approach, J. Theor. Biol. 135 (1988) 175–201.
[19] G. Bechmann, H. Weiss, P. Rich, Nonlinear inhibition curves for tight-binding inhibitors of dimeric ubiquinol-cytochrome *c* oxidoreductase. Evidence for rapid inhibitor mobility, Eur. J. Biochem. 208 (1992) 315–325.
[20] R. Covian, B.L. Trumpower, Rapid electron transfer between monomers when the cytochrome bc_1 complex dimer is reduced through center N, J. Biol. Chem. 280 (2005) 22732–22740.
[21] V.A. Shinkarev, C.A. Wraight, Intermonomer electron transfer in the bc_1 complex dimer is controlled by the energized state and by impaired electron transfer between low and high potential hemes, FEBS Lett. 581 (2007) 1535–1540.
[22] R. Covian, T. Kleinschroth, B. Ludwig, B.L. Trumpower, Asymmetric binding of stigmatellin to the dimeric *Paracoccus denitrificans* bc_1 complex, J. Biol. Chem. 282 (2007) 22289–22297.
[23] M. Castellani1, R. Covian, T. Kleinschroth, O. Anderka, B. Ludwig, B.L. Trumpower, Direct demonstration of half-of-the-sites reactivity in the dimeric cytochrome bc_1 complex: enzyme with one inactive monomer is fully active but unable to activate the second ubiquinol oxidation site in response to ligand binding at the ubiquinone reduction site, J. Biol. Chem. 285 (2010) 502–510.
[24] C.C. Moser, C.C. Page, P.L. Dutton, Darwin at the molecular, Philos. Trans. R. Soc. B 361 (2006) 1295–1305.
[25] C.C. Moser, T.A. Farid, S.E. Chabot, P.L. Dutton, Electron tunneling chains of mitochondria, Biochim. Biophys. Acta 1757 (2006) 1096–1109.
[26] C.C. Moser, J.M. Keste, K. Warnke, R.S. Farid, P.L. Dutton, Nature of biological electron transfer, Nature 355 (1992) 796–802.
[27] A.R. Crofts, Proton-coupled electron transfer at the Q_o-site of the bc_1 complex controls the rate of ubihydroquinone oxidation, Biochim. Biophys. Acta 1655 (2004) 77–92.
[28] A.R. Crofts, S. Rose, Marcus treatment of endergonic reactions: a commentary, Biophys. Acta 1767 (2007) 1228–1232.
[29] S. Lhee, D.R.J. Kolling, S.K. Nair, S.A. Dikanov, A.R. Crofts, Modifications of protein environment of the [2Fe–2S] cluster of the bc_1 complex. effects on the biophysical properties of the rieske iron–sulfur protein and on the kinetics of the complex, J. Biol. Chem. 285 (2010) 9233–9248.
[30] D.T. Gillespie, Exact stochastic simulation of coupled chemical reactions, J. Phys. Chem. 8 (1977) 2340–2361.
[31] R. Covian, E.B. Gutierrez-Cirlos, B.L. Trumpower, Anti-cooperative oxidation of ubiquinol by the yeast cytochrome bc_1 complex, J. Biol. Chem. 279 (2004) 15040–15049.
[32] P.R. Rich, The quinone chemistry of *bc* complexes, Biochim. Biophys. Acta 1658 (2004) 165–171.
[33] F. Millett, B. Durham, Use of ruthenium photoxidation techniques to study electron transfer in the cytochrome bc_1 complex, Meth. Enzymol. 456 (2009) 95–109.
[34] M.K.F. Wikström, J. Berden, Oxidoreduction of cytochrome b in the presence of antimycin, Biochim. Biophys. Acta 283 (1972) 403–420.
[35] E.C. Slater, The cytochrome b paradox, the BAL-labile factor and the Qcycle, in: V.P. Skulachev, P.C. Hinkle (Eds.), Chemiosmotic Proton Circuits in Biological Membranes, Addison-Wesley Publ. Co., Reading, Mass, 1981, pp. 69–104.
[36] J. Zhu, T. Egawa, S. Yeh, L. Yu, C.A. Yu, Simultaneous reduction of iron–sulfur protein and cytochrome b(L) during ubiquinol oxidation in cytochrome *bc*(1) complex, Proc. Natl Acad. Sci. USA 104 (2007) 4864–4869.
[37] C.-A. Yu, X. Cen, H.-W. Ma, Y. Yin, L. Yu, L. Esser, D. Xia, Domain conformational switch of the iron–sulfur protein in cytochrome bc_1 complex is induced by the electron transfer from cytochrome b_L to b_H, Biochim. Biophys. Acta 1777 (2008) 1038–1043.
[38] L. Esser, B. Quinn, Y. Li, M. Zhang, M. Elberry, L. Yu, C.A. Yu, D. Xia, Crystallographic studies of quinol oxidation site inhibitors: a modified classification of inhibitors for the cytochrome bc_1 complex, J. Mol. Biol. 341 (2004) 281–302.
[39] J.W. Cooley, D.-W. Lee, F. Daldal, Across membrane communication between the Q_o and Q_i active sites of cytochrome bc_1, Biochemistry 48 (2009) 1888–1899.
[40] S. Bartoschek, M. Johansson, B.H. Geierstanger, J.G. Okun, C.R.D. Lancaster, E. Humpfer, L. Yu, C.-A. Yu, C. Griesinger, U. Brandt, Three molecules of ubiquinone bind specifically to mitochondrial cytochrome bc_1 complex, J. Biol. Chem. 276 (2001) 35231–35234.
[41] S.J. Hong, N. Ugulava, M. Guergova-Kuras, A.R. Crofts, The energy landscape for ubihydroquinone oxidation at the Qo-site of the bc_1 complex in *Rhodobacter sphaeroides*, J. Biol. Chem. 274 (1999) 33931–33944.
[42] A.R. Crofts, S.J. Hong, N. Ugulava, B. Barquera, R.B. Gennis, M. Guergova-Kuras, E. Berry, Pathways for proton release during ubihydroquinone oxidation by the bc_1 complex, Proc. Natl Acad. Sci. USA 96 (1999) 10021–10026.